C. R. Palevol 12 (2013) 149–158

Contents lists available at SciVerse ScienceDirect

Comptes Rendus Palevol

www.sciencedirect.com

General palaeontology, systematics and evolution (Invertebrate palaeontology)

X-ray computed tomography: A promising tool to investigate the brachiopod shell interior. Effects on 3D modelling and taxonomy

La tomographie à rayons X : un outil prometteur pour l'investigation des coquilles de brachiopodes. Modélisation 3D et impact taxonomique

Danièle Gaspard

Université Paris-Sud, faculté des sciences d'Orsay, département des sciences de la Terre, 15, rue Georges-Clémenceau, Bât. 504, 91405 Orsay cedex, France

ARTICLE INFO

Article history:
Received 20 September 2012
Accepted after revision 27 January 2013
Available online 20 April 2013

Presented by Philippe Taquet

Keywords:
Brachiopod
X-ray CT
Brachidium
3D imagery
Taxonomy
Diagenesis
Collections

ABSTRACT

Barremian and Cenomanian rhynchonelliform brachiopods, one Santonian and one Holocene species (Rhynchonellida and Terebratulida), have been observed using X-ray Computed Tomography in order to investigate the shell interior. Compared to transverse serial sections used formerly, X-ray CT is a promising tool. It permits 3D modelling of the brachidium, which is important for brachiopod classification. Four types of brachidium present during the Cretaceous have been observed (crura for the Rhynchonellida, short loop for Terebratulidina–Terebratulidae, ring-loop for Terebratulidina–Cancellothyrididae and long-loop for Terebratellidina), as well as relationships lophophore/brachidium in a Holocene species. Limitations are discussed, including the nature of the sediments enclosed between the valves, diagenesis, and the necessity to observe several age groups concerning the Terebratellidina. Finally, this non-destructive tool facilitates 3D reconstruction of inaccessible brachidia to improve brachiopod taxonomy and as an aid in curating collections.

Mots clés :
Brachiopodes
Tomographie à rayons X
Brachidium
Modélisation 3D
Taxonomie
Diagenèse
Collections

RÉSUMÉ

Des brachiopodes rhynchonelliformes du Barrémien et du Cénomanien, une espèce du Santonien et une de l'Holocène (Rhynchonellida et Terebratulida) ont été examinés en tomographie à rayons X en raison des possibilités offertes par cette technique dans l'investigation des caractéristiques internes des coquilles. Comparée à l'utilisation des sections sériées transversales, la tomographie à RX est un outil prometteur, qui permet une modélisation 3D du brachidium, important dans la classification des brachiopodes. Quatre types de brachidium fréquemment observés au Crétacé – crura (Rhynchonellida), boucle courte avec et sans anneau (Terebratulidina) et boucle longue (Terebratellidina) –, ainsi que les relations du lophophore avec son support chez une espèce actuelle, sont examinés. Les limites de la méthode sont discutées : nature du sédiment inclus entre les valves, diagenèse et nécessité d'observer plusieurs classes d'âge pour les Terebratellidina. Enfin, les points positifs sont soulignés : modélisation 3D du brachidium sans destruction de coquille, évaluation taxonomique et aide à la conservation des collections.

E-mail address: ds.gaspard@orange.fr

1631-0683/$ – see front matter
http://dx.doi.org/10.1016/j.crpv.2013.01.005

1. Introduction

Following uses in the medical sciences, applications of X-ray CT increased in a range of fields, including the geological sciences (Ketcham and Carlson, 2001; Ketcham and Hanna, 2011; Tuller et al., 2011), ore geology (Kyle and Ketcham, 2003), petrology and mineralogy (Whitney and Seaton, 2010), and subsequently palaeontology.

The significance of 3D modelling is evident in palaeontology, where it was first applied to vertebrates and palaeoanthropology, and more recently through many papers in a special issue of *C. R. Palevol* concerning 3D imaging (Clément and Geffard-Kuriyama, 2010). Other examples are reported on the CT web site of the University of Texas. Micropalaeontology and invertebrate palaeontology, in a limited manner, have exploited this tool for different aspects, including general palaeontology (Garwood and Sutton, 2011), taphonomy (Lukeneder and Lukeneder, 2011), insects in amber (Soriano et al., 2010), rudists (Molineux et al., 2007), and brachiopods, focussing on soft parts (Sutton et al., 2005) or on microdetails and aspects of the brachidium (Pakhnevich, 2010; Motchurova-Dekova and Harper, 2010; Gaspard et al., 2011a,b).

X-ray CT would seem to be an interesting tool for brachiopod taxonomy. For this purpose, focus should be on the characteristics of the shell interior, particularly the brachidium (for fossils) and the relationships between the brachidium and the soft parts (for recent specimens). In addition, it is of considerable interest to combine this tool with observations using the scanning electron microscope (SEM) for details at appendix surfaces and in the shell thickness (Gaspard, 1988). In fact, the micro and nano X-ray CT provide data from the surface to the interior of both fossil and recent shells whose interest concerns the vital importance of the brachidium for brachiopod classification (Williams et al., 1996).

Brachiopods, suspension-feeding benthic marine invertebrates, are composed of a pair of bilaterally symmetrical calcite valves: pedicle (ventral) and brachial (dorsal) (Fig. 1A). Although in recent specimens, the two valves may be separated and the soft parts removed to observe the brachidium, for fossil brachiopods, unless favourable circumstances result in separated dorsal valves that are empty or filled with soft sediments (Fig. 1B, C), the brachidium remains inaccessible. It is hidden in the sediment enclosed between the two firmly articulated valves (in rhynchonelliforms). In this case, classical investigation requires transverse serial sections, after inclusion in a resin, illustrated in Kaesler (1997–2006) and commonly used in past studies (see among many authors Ager, 1965; Gaspard, 1988; Muir-Wood, 1953 and references quoted therein, Alvarez and Brunton, 2008).

Based on transverse serial sections, attempts at volumetric reconstructions of the brachidium have been realized in the past using cellulose acetate peels or plastic plates (unpublished data for teaching) or other approaches (among authors, Laurin, 1984, fig. 44). But, because it is necessary to return the block of resin to the same position following study of each section, errors are inevitably introduced during relocation and these tend to distort the 3D modeling. Furthermore, about 30 to 50 sections are obtained using this classical method, compared with several hundreds using X-ray CT. Moreover, the previous technique is destructive, whereas the high energy X-ray CT is a non-destructive tool for observing the interior structures of the shells favoring 3D modeling. However, this tool does have its limitations in spite of the outstanding qualities of this method.

2. Material and methods

Certain Cretaceous rhynchonelliform brachiopods from the Barremian and the Cenomanian stratotype regions (France) (Gaspard, 2010, 2011 submitted) as well as one Senonian and one Holocene species have been studied using X-ray CT to illustrate different types of brachidium (Fig. 2). These are described and related to their taxonomic positions.

Terebratulina biauriculata d'Orbigny (Terebratulida, Terebratulidina, Cancellothyridoidea) from the Barremian

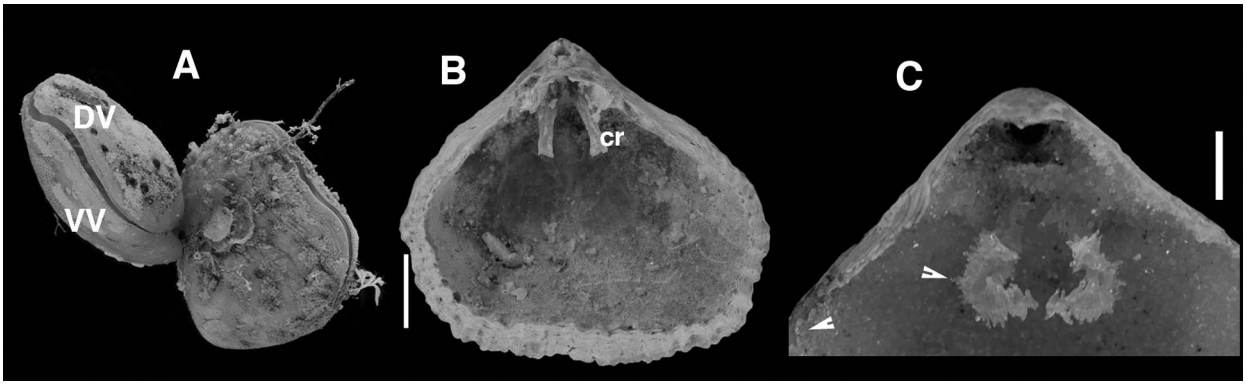

Fig. 1. **A**: Holocene rhynchonelliform brachiopod attached in living position (DV: dorsal valve, VV: ventral valve); **B**: Empty ventral valve of *Cyclothyris compressa* (Lamarck), Sarthe, articulated with the posterior part of the dorsal valve showing the brachidium (cr: crura); **C**: Empty dorsal valve of *Sellithyris cenomanensis* Gaspard, Sarthe, with the brachial loop encrusted with a lining of calcite crystals (arrow heads). Scale bar = 5 mm.
Fig. 1. **A** : Brachiopode rhynchonelliforme de l'Holocène, fixé sur un congénère, en position de vie (DV : valve dorsale, VV : valve ventrale) ; **B** : Valve ventrale vide de *C. compressa* (Lamarck), Sarthe, articulée à la partie postérieure de la valve dorsale montrant le brachidium (cr : crura) ; **C** : Valve dorsale vide de *S. cenomanensis* Gaspard, Sarthe, montrant la boucle brachiale incrustée de cristaux de calcite (tête de flèche). Échelle = 5 mm.

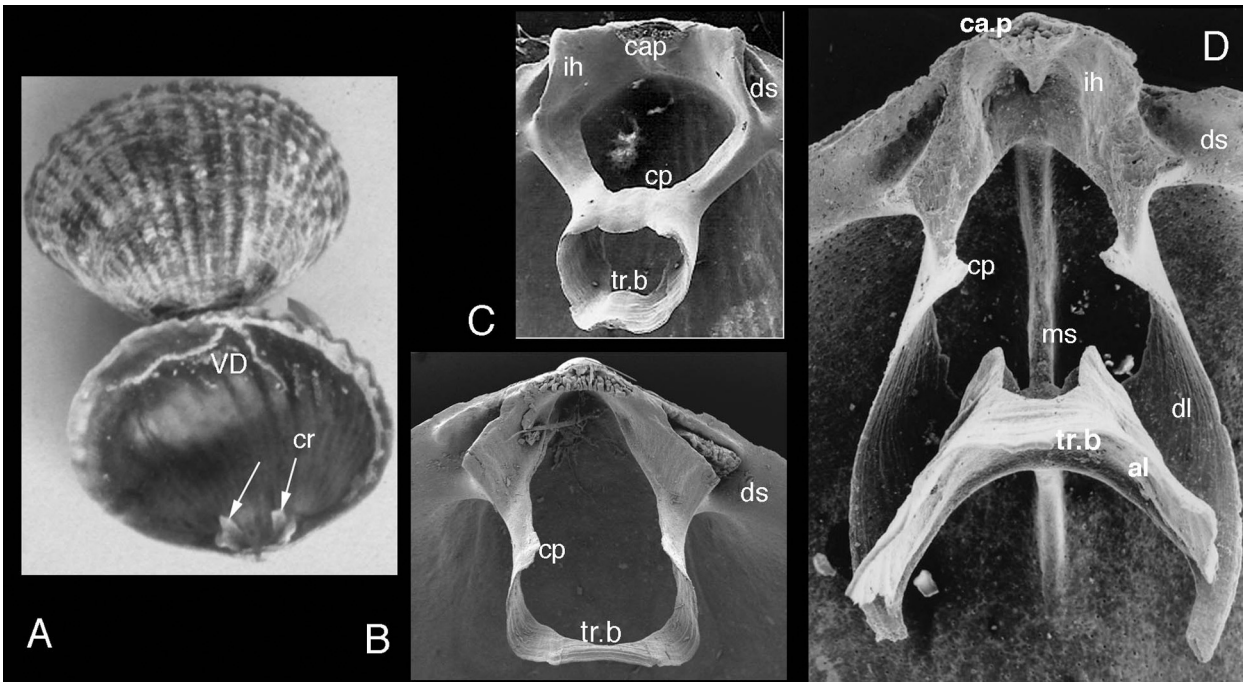

Fig. 2. Four types of brachidium in Holocene rhynchonelliform brachiopods. **A**: Rhynchonellida (cr: crura). **B–D**: Terebratulida–**B**: Short loop in Terebratulidae. **C**: Ring-loop of Cancellothyrididae. **D**: Long-loop of Kingenidae (al: ascending lamellae, ca.p: cardinal process, cp: crural process, dl: descending lamellae, ds: dental socket, ih: Inner hinge plate, ms: dorsal median septum, tr.b: transverse band).
Fig. 2. Quatre types de brachidium chez des brachiopodes rhynchonelliformes de l'Holocène. **A** : Rhynchonellida (cr : crura). **B–D** : Terebratulida–**B** : Boucle courte chez les Terebratulidae. **C** : Boucle courte avec anneau chez les Cancellothyrididae. **D** : Boucle longue chez les Kingenidae (al : branche ascendante, ca.p : processus cardinal, dl : branche descendante, ds : fossette dentale, ih : bord interne de plaque cardinale, ms : septum médian dorsal, tr.b : bandelette transverse).

(Fig. 3A) required a 3D reconstruction of the brachidium in order to place the species in the appropriate subfamily following observation of the shape (complete/incomplete) and position (low or high-pitched) of the ring.

Two rhynchonellids are compared according to the morphology of their crura:

Orbirhynchia boussensis Owen, (Rhynchonellida, Pugnacoidea, Basiliolidae) from "Les Sables de Bousse", Upper Cenomanian, Bousse, Sarthe (France) (Fig. 3B) and *Cyclothyris compressa* (Lamarck), (Rhynchonellida, Hemithiridoidea, Cyclothyrididae) from "Les Sables du Perche", Mid. Cenomanian, Le Mans, Sarthe (Fig. 3C).

One short-looped brachiopod: *Sellithyris cenomanensis* Gaspard, (Terebratulida, Terebratulidina, Terebratuloidea, Sellithyrididae) from the 'Jalais level' in the upper part of "Les Sables et Grès du Mans", Mid. Cenomanian, Le Mans, Sarthe (Fig. 3D).

Two long-looped brachiopods are examined with the purpose of emphasizing the possible relationships between the brachial loop and the dorsal median septum: *Kingena arenosa* (d'Archiac) (Terebratulida, Terebratellidina, Kingenoidea, Kingenidae), from "la Craie à *Codiopsis doma*", Lower Cenomanian, Coudrecieux (Fig. 3E) and *Gemmarcula carantonensis* (d'Orbigny) (Terebratellidina, Laqueoidea, Terebrataliidae), from "la Craie à *Carantonensis*", Upper Cenomanian, Duneau, Sarthe.

Rhynchonella vespertilio (Brocchi), (Rhynchonellida, Cyclothyrididae) from "la Craie de Villedieu" La Bouchardière Member, Santonian, Dissay-sous-Courcillon (Sarthe), has also been examined and the morphology of its crura compared with that of the two previous Cenomanian rhynchonellid species (Fig. 3F).

In addition, a specimen of *Terebratulina retusa* Linné, (Terebratulidina, Cancellothyridoidea), Holocene, from Firth of Lorn, (Scotland) enabled both comparison with *Terebratulina biauriculata* and the observation of relationships between the lophophore and its support.

The aim of this study is the construction of a three dimensional model of the brachidium that allows us to ascertain the taxonomic position of the observed specimens previously defined only from their external morphology.

The scanned images were acquired using the high-energy desktop industrial system Skyscan 1172© (Kontich, Belgium), 1173© (University of Lausanne, Switzerland), and the Vtomex© L240-180 from GE Sensing and Inspection Technologies Phoenix X-ray, used in the field of natural sciences for its wide range of applications. This latter equipment, combining two interchangeable X-ray tubes (a directional microfocus 240 kV/320 W with 1 μm of detectability, and a transmission nanofocus 180 kV/15 W with 0.5 μm of resolution), coupled with a wide-size detector, give a series of images from samples of various sizes and densities with a limit of resolution of 0.2 μm (based on the AST-RX platform, Muséum national d'histoire naturelle (MNHN), Paris).

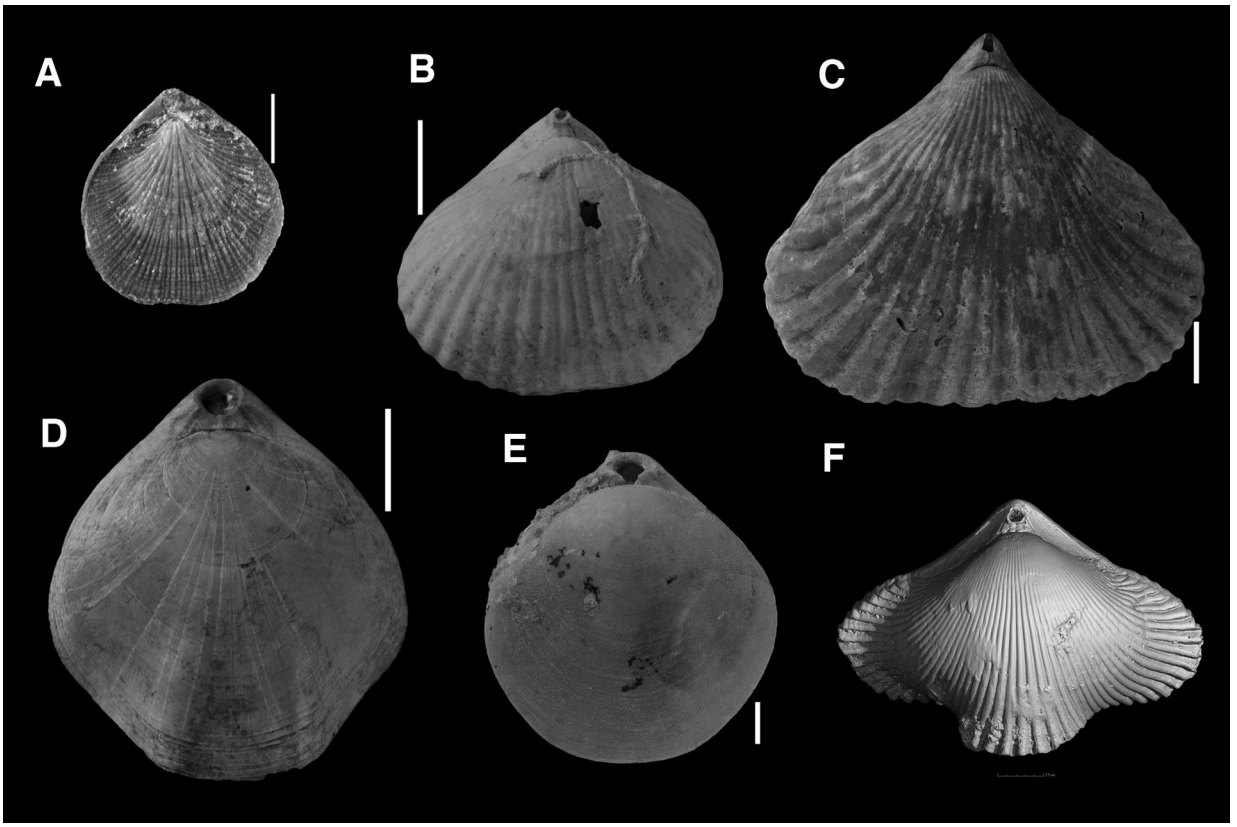

Fig. 3. **A**: *Terebratulina biauriculata* d'Orbigny, Barremian, Monclus, SE. France. **B**: *Orbirhynchia boussensis* Owen, "Sables de Bousse", Upper Cenomanian, Bousse (Sarthe, France). **C**: *Cyclothyris compressa* (Lamarck), "Sables du Perche", Cenomanian, Coulaines, Sarthe. **D**: *Sellithyris cenomanensis* Gaspard, "Jalais level", Mid. Cenomanian, le Mans (Sarthe). **E**: *Kingena arenosa* (d'Archiac), Mid. Cenomanian, Sarthe. **F**: *Rhynchonella vespertilio* Brocchi, Santonian, "La Craie de Villedieu", la Ribaudière Member, Dissay-sous-Courcillon (Sarthe); scale bar = 5 mm.
Fig. 3. **A** : *Terebratulina biauriculata* d'Orbigny, Barrémien, Monclus, SE. France. **B** : *Orbirhynchia boussensis* Owen, « Sables de Bousse », Cénomanien supérieur, Bousse (Sarthe, France). **C** : *Cyclothyris compressa* (Lamarck), « Sables du Perche », Cénomanien, Sarthe. **D** : *Sellithyris cenomanensis* Gaspard, « Niveau Jalais », Cénomanien moyen, Le Mans, Sarthe. **E** : *Kingena arenosa* (d'Archiac), Cénomanien moyen, Sarthe. **F** : *Rhynchonella vespertilio* Brocchi, Santonien, « La craie de Villedieu », membre de la Ribaudière, Dissay-sous-Courcillon (Sarthe) ; échelle = 5 mm.

The radio-transparent substrate, on which the specimen is positioned, is adjusted to correspond to the axis of the X-ray beam. Radiographic projections are made following parameters of tension (allowing us to cross the sample), intensity (contrast), power, resolution, and time exposure. A complete radiographic volume is thus obtained.

Two of the specimens were scanned at the MNHN, Paris: *Terebratulina retusa* (resolution: 12 μm; tension: 80 kV, intensity: 540 μA; time exposure: 15 min) and *Rhynchonella vespertilio* (resolution: 16 μm, tension: 70 kV; intensity: 570 μA; time exposure: 15 min). Others were scanned at the Institute of Mineralogy, University of Lausanne, Switzerland (resolution: 8–20 μm, tension: 130 kV, intensity: 60 μA, time exposure: 20 min and brass filter).

Following the acquisition of radiographic volume, a 2D reconstruction of the slices (or sections) is made (Fig. 4). Several algorithms of reconstruction permit one to improve the results by limiting or removing possible artefacts, including beam hardening and ring-artefacts (Ketcham, 2006; Ketcham and Hanna, 2011; Remeysen and Swennen, 2006). Diverse orientations of the 2D slices can be obtained. Many programs allow the reconstruction, 3D modelling, and movies, using the SkyScan 1173© and 1172© (NRECON©, TCONV©, CTvox©, DATAVIEWER©, CTVol©) and/or the Vtomex©, with in addition: MIMICS©, Cinema 4D©, VG Studio Max 2.1©.

The size of the investigated shells is from 1 cm to less than 5 cm in length.

3. Results

Concerning the Cretaceous rhynchonelliforms, four frequent types of brachidium were examined in order to reveal the articulation, various brachial length, different hinge shapes, and the morphology of the crura. The first concerns the crura (falciform, raduliform...) within Rhynchonellida (Fig. 2A). The second represents a short loop with a diversely wide and arched transverse band, and crural processes of variable length that are more or less inclined to the median symmetry plane (Terebratulida, Terebratulidina, Terebratuloidea, Fig. 2B). The third also revealed a short loop with possible connecting crural processes forming a ring with the transverse band (Terebratulidina, Cancellothyridoidea, Cancellothyrididae,

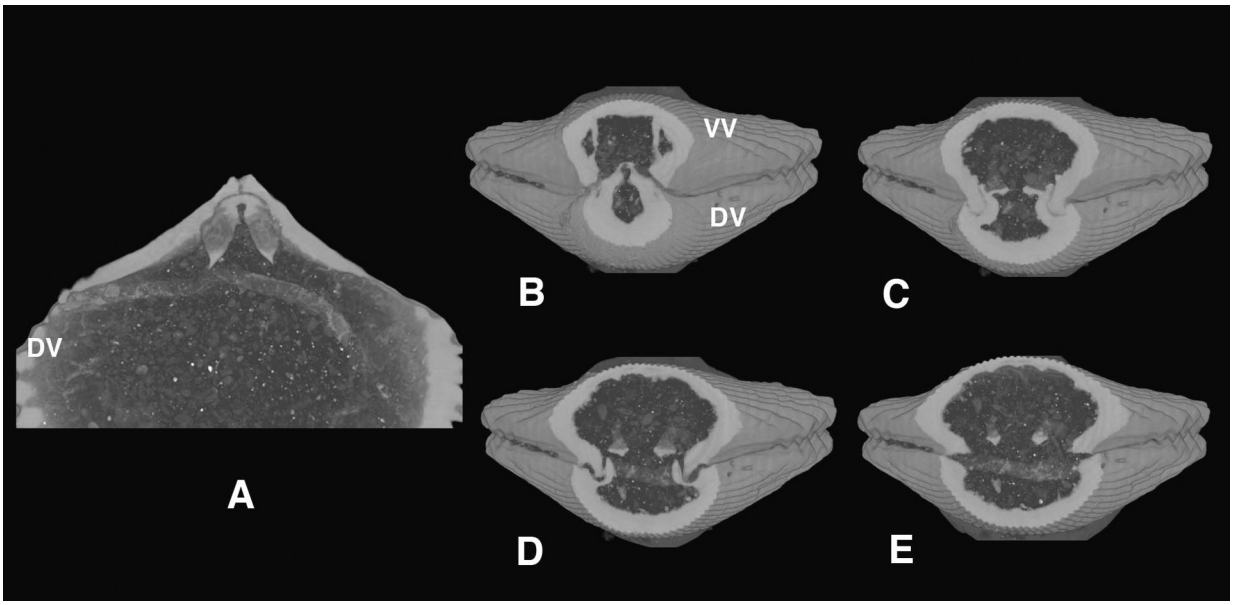

Fig. 4. *Cyclothyris compressa* (Lamarck). **A**: Dorsal valve interior, virtual sagittal view with the brachidium. **B–E**: Selected virtual transverse sections of the same specimen to reveal the details of the shell interior using CTvox©, from the dental plates to the crura, (DV: dorsal valve, VV: ventral valve).
Fig. 4. *Cyclothyris compressa* (Lamarck). **A** : Valve dorsale en vue sagittale virtuelle avec le brachidium. **B–E** : Sélection de sections transversales virtuelles du même spécimen, révélant les details des caractères internes de la coquille avec CTvox©, des plaques dentales jusqu'aux crura, (DV : valve dorsale, VV : valve ventrale).

Cancellothyridinae, Fig. 2C). The last concerns long loops attached to the median septum in mature stages (Terebratellidina, Kingenoidea (Fig. 2D), and Terebrataliidae, Gemmarculinae). The latter poses a problem because modifications occur during ontogenesis that involve several observations in relation to the age groups; this problem will be discussed below.

While the X-ray CT is a promising tool to image the inaccessible internal structure of fossil brachiopods, it facilitates identification of the different parts of the brachidium in a series (usually several hundreds) of tomography images (Fig. 4) gathered together in short movies (using CTvox© or MIMICS©, cf. movies 1 and 2 in Gaspard et al., 2011b). Furthermore, global structures can be quickly optimized and visualized using software such as MIMICS© (see fig. 4, in Gaspard et al., 2011b) or VG Studio Max 2.1© (with anaglyph relief rendering). Coloration proved to be instructive in highlighting the different parts of the shells and/or internal structures using MIMICS©. In addition to the brachidium, dental plates (in the rhynchonellids), pedicle teeth and other internal features are important in terms of presence/absence, morphology, length and thickness for determining taxonomic position. For that reason, different masks, each one corresponding to a single color, are edited and applied to each relating section (Fig. 5A) (generally in the posterior quarter of dorsal valve length for Rhynchonellida, the third valve length for short-looped Terebratulidina and nearly the entire valve length for long-looped Terebratellidina).

In addition to differences that are revealed immediately concerning shell size, foramen size, deltidial plate morphology and ornamentation (Fig. 3), comparisons of the 3D shell interior of *Orbirhynchia boussensis* (Fig. 5B) and *Cyclothyris compressa* (Fig. 5C) permit one to observe the main points that separate them. The thickness of dental plates, the width and depth of dental sockets, the outer ventrally convex hinge, the crura falciform, and the lack of a dorsal median septum characterize *O. boussensis*. In contrast, the distally concave hinge plates, the canaliform to raduliform crura, and the reduced dorsal median septum characterize *C. compressa*. Comparisons with *R. vespertilio* (Fig. 5D) also reveal differences with both previous rhynchonellids, such as medium dental plates and thick teeth articulated in wide dental sockets, details highlighted with the transparency effect using MIMICS©. However, a much-reduced median septum and the morphology of the crura are details that seem to place *R. vespertilio* and *C. compressa* together, at least in the same family.

In this manner, the 3D modelling of the brachidium of *O. boussensis* (Fig. 5B), illustrates a representative of the Pamirorhynchinae subfamily with approximately thin parallel dental plates, no median dorsal septum and crura hamiform, becoming falciform anteriorly.

The external morphological aspects allow one to place *C. compressa* in the Cyclothyrididae (Fig. 3C), while the 3D modelling of the shell interior reveals (Fig. 5C) stocky dental plates posteriorly, absence of the median septum, broad hinge plates, dental sockets wider anteriorly and long canaliform to raduliform crura that place the species in the Cyclothyridinae.

In addition, the 3D model of *S. cenomanensis* valve interior reveals (Fig. 6A, B) the dental socket shape along with small secondary sockets, the thin teeth, a bilobate cardinal process, medium crural processes, and a widely arched

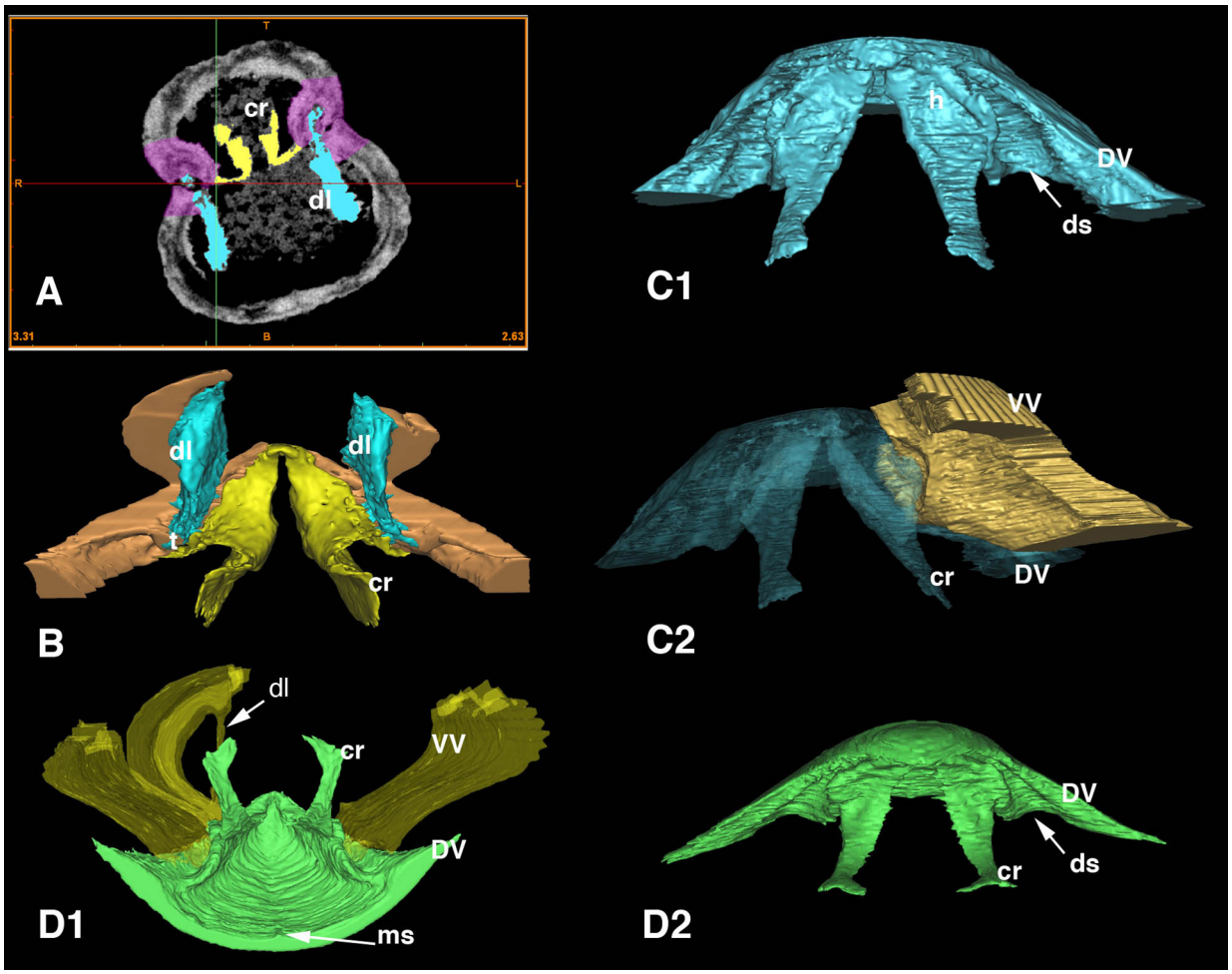

Fig. 5. A: Screen shot of a colored transverse section of *Orbirhynchia boussensis* using MIMICS© (blue: dental lamellae and teeth, pink: shell with the dental socket, yellow: hinge plates and crura). **B**: 3D representation of the posterior shell interior of *O. boussensis*. **C1–2**: 3D modelling of the brachidium of *C. compressa*, dorsal valve only (1), articulation with part of ventral valve using transparency (2). **D1–2**: 3D modelling of the posterior shell interior of *Rhynchonella vespertilio* using MIMICS©, articulation using transparency (1), with dorsal valve only (2) (DV: dorsal valve, VV: ventral valve, cr: crura, dl: dental plates, ds: dental socket, h: hinge plate, ms: light septum, t: teeth).

Fig. 5. A : Capture d'écran d'une section transversale d'*Orbirhynchia boussensis* en partie colorée, utilisant MIMICS© (bleu : lamelles dentales et dents pédonculaires, rose : partie de coquille avec les fossettes dentales, jaune : cardinalia et crura). **B** : Représentation 3D de la partie interne postérieure de coquille de *O. boussensis*. **C1–2** : Modélisation 3D du brachidium de *C. compressa*, valve dorsale seule (1), partie de valve ventrale articulée à la valve dorsale (2). **D1–2** : Modélisation 3D de la partie postérieure interne de la coquille de *Rhynchonella vespertilio*, utilisant MIMICS©, transparence utilisée au niveau de l'articulation (1), valve dorsale seule (2) (DV : valve dorsale, VV : valve ventrale, cr : crura, dl : plaques dentales, ds : fossette dentale, h : plaques cardinales, ms : faible septum, t : dents).

and moderately high transverse band, all of which place the species in the Sellithyridinae.

The CT tool proved to be useful in determining the taxonomic position of *Terebratulina biauriculata*. At first sight, the global 3D model (Fig. 6C) reveals a complete ring formed by the transverse band and the fused crural processes and relatively vertical inner hinge plates, placing *Terebratulina biauriculata* in the subfamily Cancellothyridinae. This ring can be compared with that of *Terebratulina retusa* (Figs. 2C and Fig. 7) and, because this latter species is recent, it enables one to observe the relationships between the brachidium and the lophophore and the disposition of the soft tissues using VG Studio Max 2.1© (Fig. 7D). This latter program also gives a spectacular volume rendering using the anaglyph effect (Fig. 8).

Long-looped brachiopods exemplified by *Kingena arenosa* reveal the weakness of the often partly broken loop (Fig. 9A, C). Due to the matrix heterogeneity (coarse on one side, fine on the other side), the loop has been damaged (transverse band and lamellae observed on one shell side). The program Cinema 4D© previously used in palaeoanthropology (Vialet et al., 2010) enables restitution of symmetry for this 3D model (Fig. 9B). The inner hinge plates are united to form a septalium (Fig. 9A, B). The adult loop, attached to a long, thin and high median septum (Fig. 9B, C), reveals mediovertical connecting-bands;

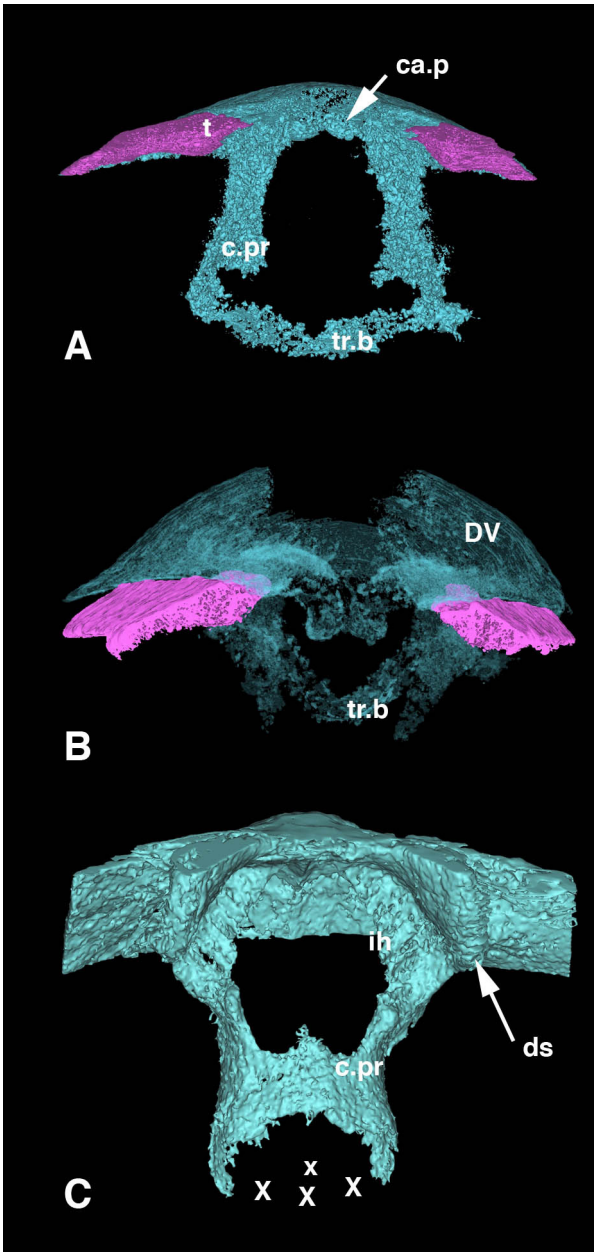

Fig. 6. A, B: 3D modelling of the brachidium of *Sellithyris cenomanensis*, with MIMICS©. **A**: Ventral view. **B**: Posterior view of the dorsal valve. **C**: 3D modelling of the brachidium of *Terebratulina biauriculate*, (cpr: crural process, ds: dental socket, ih: inner hinge plate, t: teeth, tr.b: transverse band, XXX: broken part of the transverse band).
Fig. 6. A, B : Représentation 3D du brachidium de *Sellithyris cenomanensis* avec MIMICS©. **A** : Vue ventrale. **B** : Vue postérieure de la valve dorsale. **C** : Représentation 3D du brachidium de *Terebratulina biauriculata*, (cr : processus crural, ds : fossette dentale, ih : plaque cardinale interne, t : dent pédonculaire, tr.b : bandelette transverse, XXX : partie cassée de la bandelette transverse).

thus the characteristics of the Kingeninae are identified.

Gemmarcula carantonensis, like its sister species *G. menardi* (Lamarck) are difficult also to model because the long loop is often broken and shifted. The adult specimens investigated with SkyScan 1172©, but not presented here, reveal strong dental plates, an important cardinal process and relation of the median septum with the loop using DataViewer© and/or CTvox©.

4. Discussion – Conclusion

In spite of the restrictive arguments in the use of X-ray CT compared to the synchrotron radiation X-ray tomographic microscopy (Motchurova-Dekova and Harper, 2010, p.110, 113), the X-ray CT appears to be a promising tool with which to investigate the interior of brachiopod shells (see Pakhnevich, 2010 and references quoted therein; Gaspard et al., 2011a,b). For palaeontologists, the desktop instruments (SkyScan) are more accessible tools for routine examination as well as the Vtomex© than the synchrotron apparatus. However, the method has certain limitations. The quality of results depends largely on the time required for post treatment of initial scanned images and virtual slices, to mitigate the artifacts and to elaborate optimal 3D images of the internal structures, particularly of the brachidium.

4.1. Limitations

Limits to this application concern the machine and others inherent to the material observed. Resolution is limited according to the diameter of the shell section, and, in the case of extreme resolution, the boundaries of the material investigated can be blurred. The specimen size may also be an obstacle, sometimes too large for the nano-CT or insufficiently large for the micro-CT (Vtomex© L240-180). Artefacts susceptible to complicate the data acquisition are the "ring artefacts" (see Pakhnevich, 2010, pl. 4, fig. 12–14), which may be corrected (Ketcham, 2006; Ketcham and Hanna, 2011), and the phenomenon of "beam hardening" (cf. Remeysen and Swennen, 2006).

It may not be easy to obtain a convenient grey calibration (cf. contrast), depending on the nature of the shell, infilling sediment and possible diagenetic modifications. In some cases shells are empty, like geodes, encrusted with a lining of calcite crystals (Fig. 1C) or other calcite or siliceous replacements that may deform certain aspects in the 3D modeling of the brachidium (Fig. 6A, C). The nature of the sediment compared with that of the brachiopod shell may also pose problems, i.e. it is difficult to obtain sufficient contrast for a correct imagery when carbonate matrix is enclosed between the low-Mg calcite valves. In other cases it is impossible to obtain correct 2D imagery because the sediment is very fine with uniform density. However, positive results have been obtained with shells filled with marls (it is the case for *Terebratulina biauriculata*) and with detrital sediments (*S. cenomanensis* and/or *C. compressa*). Broken brachidia and sediment composition may complicate the method.

Intrinsic properties of some structures like long loops may also raise problems. This kind of loop is more fragile and reveals significant modifications during ontogenesis. The long-looped species, illustrated here by *Kingena arenosa* (d'Archiac), reveals relationships between the loop

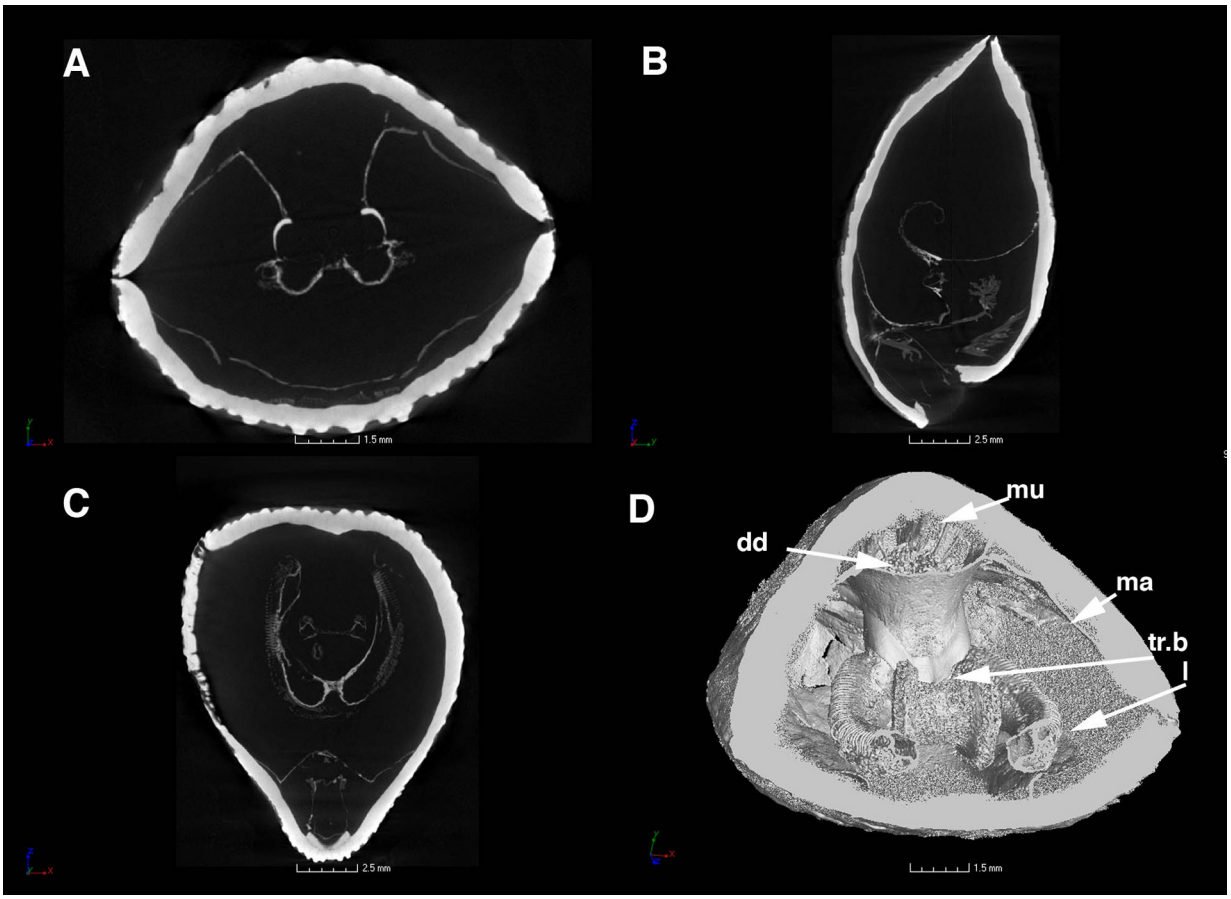

Fig. 7. *Terebratulina retusa* Linné, screen shot using VG Studio Max 2.1©. Virtual transverse (**A**), longitudinal (**B**) and sagittal slices (**C**). **D**: Volume rendering of a *T. retusa* shell, with virtually removed oblique anterior part, illustrating the relationships between the lophophore and its support (l) and, revealing the location of muscles (mu), digestive diverticules (dd) and mantle shell (ma).
Fig. 7. *Terebratulina retusa* Linné, capture d'écran avec VG Studio Max 2.1©. Sections virtuelles transversale (**A**), longitudinale (**B**), sagittale (**C**). **D** : Modélisation 3D de la coquille, virtuellement coupée dans sa partie antérieure, illustrant les relations entre le lophophore et son support (l) et l'emplacement des muscles (mu), des diverticules digestifs (dd) et du manteau de la coquille (ma).

and the dorsal median septum. The specimen illustrated represents an adult stage. It is necessary to investigate different age groups in order to see when the attachment operates or disappears. Similarly, observations of Holocene Antarctic species such as *Magellania joubini* Blochmann and/or other long-looped species including *Macandrevia africana* Cooper and *Ecnomiosa inexpectata* Cooper (species not figured in the present paper) illustrate this point. In certain species the adults have an attached loop but the juveniles do not, but the reverse condition also exists. Beecher (1893) has emphasized different types of brachial structures presented according to family importance, and Richardson (1975) gave a schematic representation of the loop development in certain families. Concerning this subject, Gaspard (2003) illustrated the result of ontogenetic evolution by which some mature loops proceed, confirming the necessity to observe several age groups by using the X-ray CT tool. However, the weakness of ascending and descending branches of this kind of loop is a real problem in the fossil record and this complicates the 3D modeling, illustrated here by *K. arenosa* and the successful use of Cinema 4D© to construct symmetrical parts. It is also the case for many specimens of *Gemmarcula menardi* (Lamarck) and *G. carantonensis* (d'Orbigny) from the Cenomanian stratotype, generally found with broken loops using SkyScan 1172© (see Gaspard, 2011, fig. 8F for an example). These last examples emphasize the fact that this promising tool is also an expensive technique (when it is necessary to renew the observations and investigate many age groups) depending also on the availability of machine time and cost of various programs.

4.2. Positive aspects

The author emphasises the importance of this technique for curating Museum collections, especially for type and figured specimens, leading to a valorisation of the collections (see among authors, Garcia Sanz et al., 2012; Motchurova-Dekova and Harper, 2010; Pakhnevich, 2010).

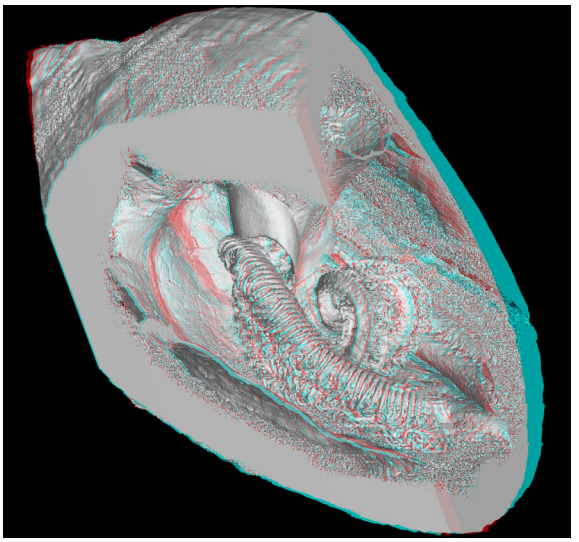

Fig. 8. 3D modelling of a *Terebratulina retusa* shell using VG Studio 2.1© (anaglyph effect, needs appropriate glasses to be observed) with virtually removed lateral and dorsal slices. Relationships between the lophophore and its support, and location of soft tissues are revealed (compared with Fig. 7D).
Fig. 8. Modélisation 3D de la coquille de *Terebratulina retusa* avec l'aide de VG Studio 2.1© (effet anaglyphe, nécessite des lunettes appropriées pour une meilleure observation) avec des parties virtuellement enlevées. Les rapports du lophophore avec le brachidium et l'emplacement des tissus mous sont ainsi mis en évidence (comparer avec la Fig. 7D).

No major preparation is required for this non-destructive tool, which provides details at a subvoxel level. Many available programs, favoring enhancement of different parts of the shell interior, are presented using different colors and/or transparency (dental lamellae, pedicle teeth, dental sockets, relations of both valves, crura. . .). A quick 3D model of the brachidium is thus available (with MIMICS©) allowing a rapid taxonomic decision; the case of *Terebratulina biauriculata* illustrates this method (Gaspard et al., 2011b, fig. 4). Virtual sections (longitudinal, sagittal and transversal) have been obtained using DATAVIEWER© and CTvox© (Fig. 4A–E) and VG Studio Max 2.1©. Movies are obtained using different programs including MIMICS©, allowing one to visualize the brachidium on all faces (ventrally, in profile, dorsally or in inclined plane, see movies 1 and 2 in Gaspard et al., 2011b) and to explore the shell interior through virtual slices from the posterior to the anterior part with CTvox©. The use of anaglyph, in VG Studio Max 2.1©, applied to recent shells (see *Terebratulina retusa*) gives a spectacular relief clarifying the relationships between the lophophore and its support, as well as the location of the soft tissues using appropriate glasses (Fig. 8). The examples illustrated show that X-ray CT is a promising tool from several points of view, especially for investigating the interior of brachiopod shells, its modifications during ontogenesis and variations in a single population or between populations. This method may lead to improve taxonomic precision, facilitate teaching, and help in curating collections.

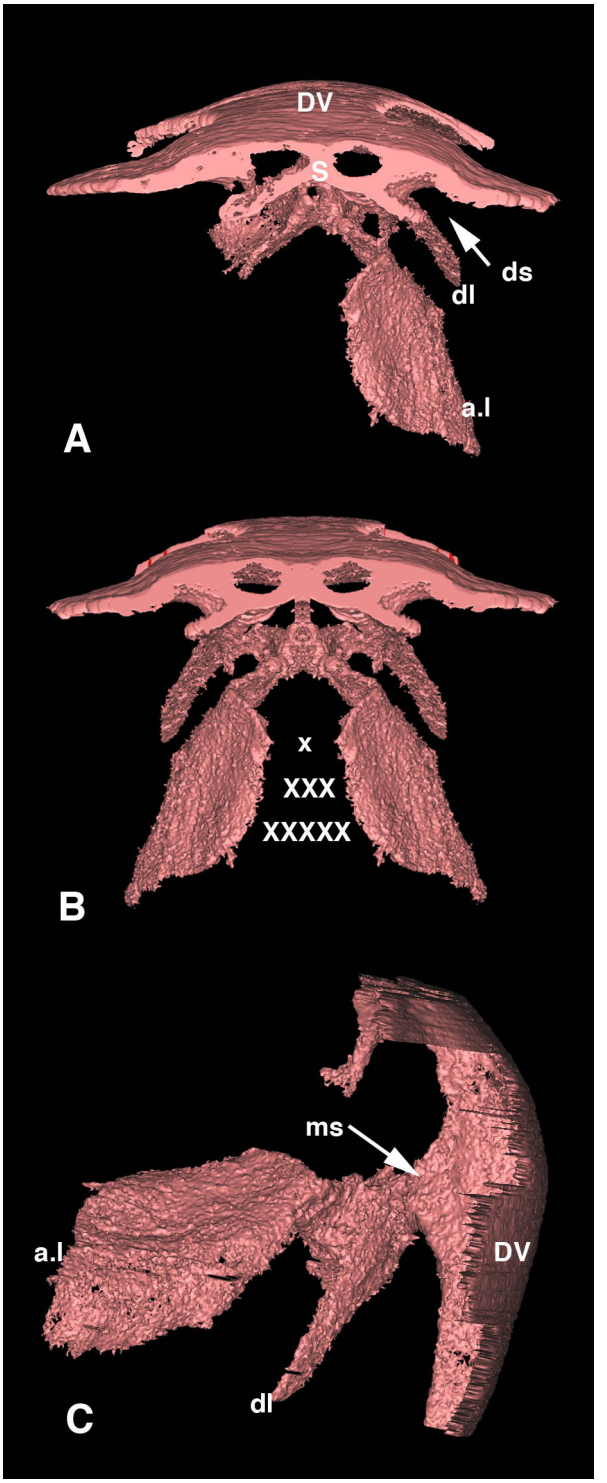

Fig. 9. 3D modelling of *Kingena arenosa*. **A**: Brachial loop partly broken using MIMICS©, posterior view. **B**: Symmetry construction using Cinema 4D© (XXX: in place of the broken transverse band). **C**: In profile to observe the attachment with the median septum (ms).
Fig. 9. Modélisation 3D du brachidium de *Kingena arenosa* avec MIMICS©. **A** : Boucle brachiale longue en partie cassée, vue postérieure. **B** : Restitution de symétrie en utilisant Cinema 4D© (XXX : remplace la bandelette transverse manquante). **C** : Vue de profil pour apprécier l'attache avec le septum médian (ms).

Acknowledgments

I would like to thank Prof. Lukas Baumgartner and Dr. Benita Putlitz of the Institute of Mineralogy of Lausanne (Switzerland) who welcomed and helped me manipulate the SkyScan 1173, Evi Bongaert (SkyScan, Belgium) for the SkyScan 1172, Prof. Philippe Janvier who authorised the use of the AST-RX platform UMS 2700 "Outils et méthodes de la systématique intégrative, CNRS–MNHN" (MNHN, Paris) as well as Florent Goussard for his help. Thanks are also due to Nicolas Morel, curator of the collections, "Musée vert du Mans" (Sarthe, France), for the loan of Cenomanian specimens, Arnaud Clément for the Barremian specimens, Jean-Christophe Dudicourt for the Santonian specimens, and Philippe Loubry (MNHN, Paris) for images concerning Fig. 3A–E. The anonymous reviewers are thanked for their comments. I am grateful to Prof. Carl Koch (Old Dominion Univ., Norfolk) and Prof. Bruce Harold Purser (University Paris-Sud, Orsay) for revising the English writing.

References

Ager, D.V., 1965. Serial grinding techniques in Mechanical Methods of Preparation. In: Kummel, B., Raup, D. (Eds.), Handbook of Paleontological Techniques. Freeman and Co, San Francisco and London, pp. 212–224.

Alvarez, F., Brunton, C.H.C., 2008. On the reliability of reconstructing and comparing brachiopod interiors and their morphological variations based solely on serial sections. Proc. R. Soc. Victoria 120 (1), 58–74.

Beecher, Ch.E., 1893. Revision of the families of loop-bearing brachiopoda – The development of *Terebratalia obsoleta* Dall. Connecticut Academy of Arts and Sciences Transactions 9 (2), 376–399, 3 pls.

Clément, G., Geffard-Kuriyama, D., 2010. 3D et imagerie en sciences paléontologiques et paléoanthropologiques. C. R. Palevol 9, 255–470.

Garcia Sanz, M., Goussard, F., Balzeau, A., Clément, G., 2012. Imaging methodologies in natural sciences The AST-RX (Accès scientifique à la tomographie à rayons X) Platform of the Muséum d'Histoire naturelle, Paris. Oral presentation UVX 2012, Biarritz. UVX Congress, in press.

Garwood, R., Sutton, M., 2011. Tomographic reconstruction in palaeontology. EGU General Assembly 2011, Vienna. Session GI-12: "3D Modelling in Earth Sciences", Abstract 4452.

Gaspard, D., 1988. Sellithyridinae Terebratulidae du Crétacé d'Europe occidentale – Dynamique des populations systématique et évolution. Cahiers de Paléontologie CNRS Ed, 243 p, 28 pls.

Gaspard, D., 2003. Biomineralization approach vs Immunology in Brachiopod taxonomy? The loop ontogeny of some Recent Terebratulides as an example. In: Kobayashi, I., Ozawa, H. (Eds.), Biomineralization (BIOMIN 2001): formation, diversity, evolution and application. Proceedings of the 8th International Symposium on Biomineralization. Tokai Univ. Press, Kanagawa, pp. 66–70.

Gaspard, D., 2010. Brachiopodes. In: De Wever, P., Cornée, A.Dir. (Eds.), Stratotype du Barrémien, Collection "Patrimoine géologique". Coédition Muséum-Biotope-BRGM (submitted).

Gaspard, D., 2011. Brachiopodes. In: De Wever, P., Cornée, A.Dir. (Eds.), Stratotype du Cénomanien, Collection "Patrimoine géologique". Coédition Muséum-Biotope-BRGM (submitted).

Gaspard, D., Putlitz, B., Baumgartner, L., 2011a. Micro-CT for 3D reconstruction of brachiopod shells interior: an alternative to destructive serial sections. EGU General Assembly 2011, Vienna. Session GI-12: "3D Modelling in Earth Sciences". Abstract 9914.

Gaspard, D., Putlitz, B., Baumgartner, L., 2011b. X-ray computed Tomography – A promising tool for Brachiopod Shell investigations. IAMG Conference, Salzburg, 2011. Session NDA3: "Microtomography & 3D Modelling in Paleontology". IAMG publication. doi:10.5242/iamg.2011.0292, 16p + 2 movies.

Kaesler, R.L., 1997–2006. Treatise on Invertebrate Paleontology, part H: Brachiopoda Revised, 1–6. The Geological Society of America and the University of Kansas, 3226 p.

Ketcham, R.A., 2006. New algorithms for ring artifact removal. In: Bonse, U. (Ed.), Developments in X-ray tomography. Proceedings of the SPIE 6318 (631801), doi: 10.1117/12.680939.

Ketcham, R.A., Carlson, W.D., 2001. Acquisition, optimization and interpretation of X-ray computed tomographic imagery: applications to the geosciences. Comput. Geosci. 27, 381–400.

Ketcham, R.A., Hanna, R., 2011. Expert-guided CT beam hardening correction for heterogeneous natural materials. IAMG Conference, Salzburg 2011. Session NDA1: "Computed Tomography in Geosciences". IAMG publication, http://dx.doi.org/10.5242/iamg.2011.0283, 9 p.

Kyle, R., Ketcham, R.A., 2003. In-situ distribution of gold in ores using high-resolution X-ray computed tomography. Econ. Geol. 98, 1697–1701.

Laurin, B., 1984. Les Rhynchonellidés des plates-formes du Jurassique moyen en Europe occidentale–Dynamique des populations, évolution systématique. Cahiers de paléontologie, CNRS (Ed.), Paris, 465p, 14 pls.

Lukeneder, S., Lukeneder, A., 2011. Methods in 3D modelling of Triassic ammonites from Turkey (Taurus, FWF P22109-B17). IAMG Conference Salzburg, 2011. Session NDA3: "Microtomography & 3D Modelling in Paleontology". IAMG publication, http://dx.doi.org/10.5242/iamg.2011.0225, 10 p.

Motchurova-Dekova, N., Harper, D.A.T., 2010. Synchrotron radiation X-ray tomographic microscopy (SRXTM) of brachiopod shell interiors for taxonomy: preliminary report. Ann Geol. Peninsule Balkanique 71, 109–117.

Molineux, A., Scott, R.W., Ketcham, R.A., Maisano, J.A., 2007. Rudist taxonomy using X- ray computed tomography. Palaeontol. Electron. 10 (3), 13A, 6 p.

Muir-Wood, H.M., 1953. Techniques employed in grinding and illustrating serial transverse sections of fossil brachiopods. Ann. Mag. Nat. Hist. 12 6, 919–922.

Pakhnevich, A.V., 2010. Study of fossil and Recent brachiopods using a Skyscan 1172 X-ray microtomograph. Paleontol. J. 44 (9), 1217–1230.

Remeysen, K., Swennen, R., 2006. Beam hardening artifact reduction in microfocus computed tomography for improved quantitative coal characterization. Int. J. Coal Geol. 67, 101–111.

Richardson, J.R., 1975. Loop development and the classification of terebratellacean brachiopods. Palaeontology 18 (2), 285–314.

Soriano, C., Archer, M., Azar, D., Creaser, Ph., Delclòs, X., Godthelp, H., Hand, S., Jones, A., Nel, A., Néraudeau, D., et al., 2010. Synchrotron X-ray imaging of inclusions in amber. C. R. Palevol 9, 361–368.

Sutton, M.D., Briggs, D.E.G., Siveter, David, J., Siveter Derek, J., 2005. Silurian brachiopods with soft-tissue preservation. Nature 436 (3846), 1013–1015.

Tuller, M., Vaz, C.M.P., Lasso, P.O., Kulkarni, R., 2011. A new generation of high-resolution benchtop micro-CT scanners for application in Earth sciences. EGU General Assembly 2011, Vienna. Session GI-12: "3D Modelling in Earth Sciences". Abstract 5798.

Vialet, A., Guipert, D., Jianing, H., et al., 2010. *Homo erectus* from the Yunxian and Nankin Chinese sites: Anthropological insights using 3D virtual imaging techniques. C. R. Palevol 9, 331–339.

Whitney, D.I., Seaton, N.C.A., 2010. Garnet polycrystals and the significance of clustered crystallization. Contrib. Mineral. Petr. 160, 591–607.

Williams, A., Carlson, S.J., Brunton, C.H.C., Holmer, L.E., Popov, L.E., 1996. A supra-ordinal classification of the Brachiopoda. Philos. Trans. R. Soc. Lond. B Biol. Sci. 351, 1171–1193, 6 figs.